Organic Electronics 15 (2014) 1624–1630

Contents lists available at ScienceDirect

Organic Electronics

journal homepage: www.elsevier.com/locate/orgel

In-situ investigation of interfacial effects on charge accumulation and extraction in organic solar cells based on transient photocurrent studies

Xianfeng Qiao [a], Chen Zhao [a], Bingbing Chen [a], Lin Luan [a], Bin Hu [a,b,*]

[a] WuHan National Laboratory for Optoelectronics and School of Optical and Electronic Information, Huazhong University of Science and Technology, Wu Han 430074, China

[b] Department of Materials Science and Engineering, University of Tennessee, Knoxville, TN 37996, United States

ARTICLE INFO

Article history:
Received 22 January 2014
Received in revised form 2 April 2014
Accepted 14 April 2014
Available online 26 April 2014

Keywords:
Organic solar cell
Transient photocurrent
Interfacial dipole
Charge accumulation
Charge recombination

ABSTRACT

In organic solar cells, the interfacial and bulk photovoltaic processes are typically coupled based on charge transport and accumulation. In this article, we demonstrated that the in situ transient photocurrent measurements can be a powerful approach to separately investigate the interfacial effects on interfacial and bulk photovoltaic process. Based on this method, the effects of interfacial dipoles on charge extraction, accumulation, and recombination are solely studied by comparing Ca and Al devices with standard architecture of ITO/PEDOT/P3HT:PCBM/cathode. We observe that stronger interfacial dipoles can significantly decrease the charge extraction time and consequently increase the charge extraction efficiency. More importantly, stronger interfacial dipoles can also decrease the charge accumulation within the bulk photovoltaic layer. Furthermore, our experimental results indicate that the bulk-accumulated charges can act as recombination centers under device-operating condition, resulting in the recombination loss in photogenerated carriers. Clearly, our studies of transient photocurrents elucidated the charge extraction, accumulation, and recombination in OSCs.

1. Introduction

Organic solar cells (OSCs) have become a promising low-cost photovoltaic technology due to its merits of transparency, possible printing fabrication, and mechanical flexibilities [1–3]. In the last few years, the power conversion efficiencies (PCE) have largely improved exceeding 10% [4] due to the effort from materials synthesis [5–8] and device engineering [9–12]. Recent developments have shown that the organic/electrode interfacial properties are a critical component in improving photovoltaic performance [13–16]. Specifically, the interfacial properties not only directly affect the charge collection efficiency [13–17] but also strongly change charge transporting process, such as charge accumulation and recombination [18–22]. Therefore, further understanding the complex photovoltaic processes related to interfacial properties is essentially important for device performance optimization.

In OSCs, the photogenerated carriers are either collected at the respective electrodes to generate external photocurrent or recombine within the bulk-heterojunction (BHJ) layer to cause a loss [19–22]. It is worth to emphasize that the interfacial charge extraction can affect bulk charge accumulation and recombination under device-operating condition. Specifically, the charge transport occurs through bulk and interfacial channels with series connection

* Corresponding author at: WuHan National Laboratory for Optoelectronics, Huazhong University of Science and Technology, Wu Han 430074, China.
E-mail address: bhu@utk.edu (B. Hu).

http://dx.doi.org/10.1016/j.orgel.2014.04.019
1566-1199/

toward the generation of photocurrent. The bulk charge transport and interfacial charge extraction are mutually coupled in transporting photogenerated carriers. An effective interfacial extraction can lead to a less charge accumulation in a bulk photovoltaic film and consequently enhances the bulk charge transport. This can lead to a less recombination of bulk charge carriers. It should be pointed out that the dynamic effects of the interfacial charge extraction on bulk charge accumulation and recombination have not been extensively studied. In this work, we use transient technology to investigate the internally connected interfacial extraction and bulk accumulation and recombination based on conventional P3HT:PCBM solar cells. In general, transient measurements including photo-induced charge extraction by linearly increasing voltage (photo-CELIV) [23–26], transient photovoltage [27–32], and transient photocurrent [33–39] can be used to characterize interfacial properties, bulk charge trapping, and bulk recombination. In this report, we use transient photocurrent measurements to particularly investigate the influences of interfacial dipoles on surface charge extraction and bulk charge accumulation and recombination. The aluminum (Al) and calcium (Ca) cathodes with different work-function are employed to alter the interfacial dipoles [40–42]. It has been reported that the interfacial properties, such as interface gap state and chemical reaction, are different due to the difference in work-function between Ca and Al cathodes [40,43]. Ultimately, the interfacial dipole moment and energy level alignment can largely be changed when different electrodes are used.

2. Experimental section

2.1. Device preparation

The bulk heterojunction devices used in this study were based on blends containing poly(3-hexylthiophene) (P3HT) and 1-(3-methyloxycarbonyl)propyl-1-phenyl [6,6] C61 (PCBM). The high-workfunction Al and low-workfunction Ca cathodes are employed to alter the interfacial dipoles. The P3HT was purchased from Nanostructured Carbon and used as the electron donor. The PCBM purchased from Luminescence Technology was used as electron acceptor. The ITO glass substrates with a sheet resistance of 10 Ω/γ were cleaned by ultrasonic cleaning in lotion, ethanol and deionized water successively, followed by dried in an oven for 2 h. A 40 nm thick layer of poly(3,4-ethylenedioxythiophene): poly(styrenesulfonate) (PEDOT:PSS) (Baytron P AI4083) was deposited on to the oxygen plasma-treated substrates by spin-casting with 4000 rpm for 1 min, and then the PEDOT:PSS films were annealed at 150 °C for 30 min. P3HT and PCBM were co-dissolved in ortho-dichlorobenzene (ODCB) solution with a total solution concentration of 36 mg mL^{-1} and weight ratio of 1:0.8 (P3HT:PCBM). This solution was spin-coated at 1000 rpm to form 120 nm-thick blend films. The films were then transferred into a vacuum chamber for cathode deposition. The Al (100 nm) and Ca/Al (20 nm/100 nm, layer/layer configuration) electrodes were deposited under the vacuum of 2×10^{-6} Torr. The devices with Al as cathode were post-annealed while the Ca devices were re-annealed at 150 °C for 10 min in nitrogen gas. The active area determined by the cross of ITO and cathode is 0.09 cm^2 in this study.

2.2. Device testing

The photocurrent–voltage characteristics were recorded by using Keithley 2400 source meter under illumination of AM 1.5G 100 mW cm^2 from Newport solar simulator calibrated to a silicon reference cell. For transient photocurrent measurement without background illumination, a high-brightness 590 nm LED (Intelligent LED Solutions, ILH-ON04-YELL-SC201) was used as the light source and a Hewlett Packard (HP) 8114A pulse generator was used as the power source for the LED. For the transient photocurrent measurement with background illumination, a white high-brightness LED (Intelligent LED Solutions, ILH-ON04-NUWH-SC201) was used for background illumination with Keithley 2400 as power supply. The purpose of employing background light is to explore the effects of trap on photocurrent dynamics. Therefore, the light intensity should be intensity-tunable. At the same time, the pulse intensity cannot be too strong to avoid charge accumulation within the device. A silicon solar cell (Nowport 91150V) was used as the reference cell for light intensity calibration. Devices were connected in series with Agilent 33522A pulse/function generator operating in DC mode for voltage-dependent photocurrent measurements. The Tektronix DPO 4104 digitizing oscilloscope with input impedance of 1 MΩ recorded the transient photocurrent by measuring the voltage drop across an external 51 Ω resistor in series with the voltage supply and the devices.

3. Results and discussion

In OSCs, the extraction of photogenerated charge carriers is either bulk-limited by the BHJ layer properties or interface-limited by the organic/electrode interfacial properties [19–22]. To distinguish these two limited processes, we examined the photocurrent decay dynamics in short-circuit current condition as function of pulse light intensity. Fig. 1a and b display the transient photocurrent responses under a pulse photoexcitation of 500 ns square wave at 590 nm. The insets indicate the experimental data for normalized current decay characteristics with fitted curves by using a single exponential decay mode. The curve fitting gives charge extraction time $\tau_{1/e}$, shown in Fig. 1d (the details can be seen in Supporting Information). The $\tau_{1/e}$ is defined as the time for the photocurrent to decay to $1/e$ of its peak value. The pulse intensity dependence of $\tau_{1/e}$ can be then used to estimate the extraction limiting processes in OSCs. We can see in Fig. 1d that the extraction time $\tau_{1/e}$ linearly increases with pulse intensity for Al device, while the device with Ca cathode exhibits weak intensity dependence of $\tau_{1/e}$ of 0.72 ± 0.06 μs. There are two different cases, namely bulk-limited regime and interface-limited regime, to determine the dependence of light intensity on extraction time $\tau_{1/e}$. In bulk-limited regime, the charge extraction process is mainly determined by

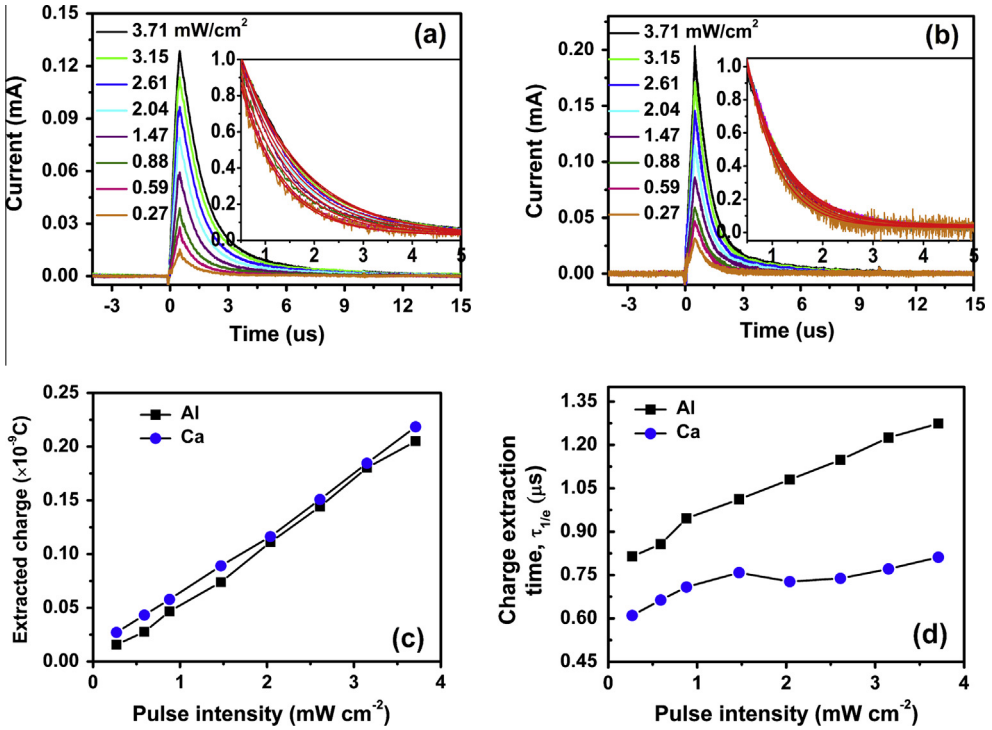

Fig. 1. Transient short-circuit photocurrent of the P3HT:PCBM devices with Al (a) and Ca (b) as cathode in response to a short 500 ns square-pulse with 590 nm wavelength for various intensities. The insets in part a and b highlight the normalized current decay normalized to the peak current value and the red lines present fits to a single exponential decay $y = A * e^{-\frac{x-x_0}{\tau}}$. (c) The amount of extracted charge in response to light intensity. (d) The dependence of extraction time on pulse intensity.

BHJ layer [15,20]. If the annealed BHJ layer is trap free, the $\tau_{1/e}$ is therefore insensitive to carrier density in absent of space charges effect [20]. In the interface-limited regime, the charge extraction is limited by interfacial barrier, thus the photogenerated carrier density will greatly affect the $\tau_{1/e}$, leading to an intensity-dependent $\tau_{1/e}$. Therefore, the pulse intensity dependence of $\tau_{1/e}$ can indicate whether the charge extraction is bulk-limited or interface-limited process. It should be pointed out that our discussions are based on the assumption of no bulk charge accumulation and trap-free transport in the active layer. To validate this assumption, we should use photoexcitation with low intensity and short pulse width. Comparing the peak current at low and high pulse intensities in Figs. 1a and 2a, we can see that the peak current at low pulse intensity does not show any saturation while a high pulse intensity leads to a saturation on transient photocurrent. Thus, it is clear that the amount of the photogenerated charge carriers is far less than the upper limit of transporting capacity of the BHJ layer at low pulse intensity. Therefore, our experimental data shown in Figs. 1a and 2a confirm that low pulse intensity used in our study can satisfy the condition: negligible bulk accumulation. Furthermore, we can see from Fig. 1d that the Ca electrode exhibits a lower extraction time compared to Al cathode at constant light intensity. For instance, at pulse intensity of 1.47 mW cm^{-2}, the $\tau_{1/e}$ values are determined to be 0.76 μs and 1.01 μs for Ca and Al devices, respectively. This experimental result provides the following two pieces of information. First, the decrease in extraction time caused by the lower work-function Ca cathode can generate a higher peak photocurrent (Fig. 1b). Second, the electrode interface can largely control the charge extraction time at low pulse intensity. It has been found that Ca with low work-function can form stronger interfacial dipoles, which can facilitates charge extraction [41–43].

At high light intensity such as 1 sun condition, the space charges within the BHJ layer also play an important role in determining device performance. Space charges mainly consist of trapped charges and accumulated charges [30]. In absent of charge trapping, the bulk charge accumulation should be accountable for space charges. Here, we further investigate the effect of interfacial dipoles on charge accumulation by transient photocurrent measurements. A photoexcitation with strong intensity and long pulse width is employed to generate bulk accumulation within the P3HT:PCBM layer. Fig. 2a and b shows the photocurrent response to the strong pulse as a function of pulse intensity. Evidence for charge accumulation within the P3HT:PCBM devices can be obtained from the dependence of $\tau_{1/e}$ on pulse intensity. As shown in Fig. 2d, the $\tau_{1/e}$ for Ca device is almost constant value below the critical light intensity of 17.6 mW cm^{-2}, and then increases with pulse intensity. In fact, this turning point at the critical light intensity of 17.6 mW cm^{-2} is an indicator of critical light intensity above which charge accumulation occurs. At pulse intensities lower than 17.6 mW cm^{-2}, the $\tau_{1/e}$ is independent on pulse intensity. This means that the charge

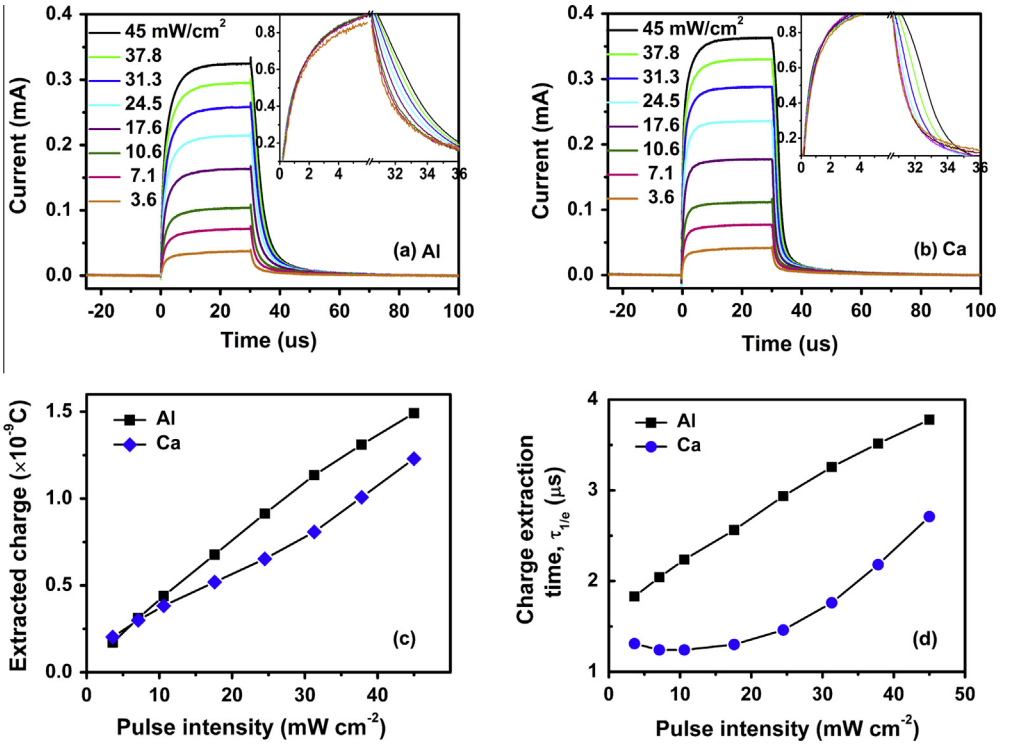

Fig. 2. Transient short-circuit photocurrent of the P3HT:PCBM devices with Al (a) and Ca (b) as cathode in response to a 30 μs square pulse with 590 nm wavelength for various intensities. The insets in part a and b highlight the rise/decay dynamics as function of light intensity. (c) The amount of extracted charge in response to light intensity. (d) The dependence of extraction time on light intensity.

extraction process is controlled by the bulk properties and the charge accumulation becomes negligible at low pulse intensity. As the pulse intensities exceeding 17.6 mW cm^{-2}, more charge are generated than the upper limit of the transporting capacity. In this case, charge accumulation take places and generates space charges at electrode interface, leading to an intensity-dependent $\tau_{1/e}$. To confirm charge accumulation indeed occurring above 17.6 mW cm^2, theoretical calculation is carried out. In the P3HT:PCBM device, the maximal density of charge carriers determined by space charges is calculated to be 1.73×10^{16} cm^{-3} at short-circuit condition, by using the hole mobility of $7.7 \times 10^{-5} cm^{-3} V^{-1} s^{-1}$ reported for P3HT:PCBM film [44]. To achieve this level of charge density in our devices, the critical intensity of the monochromatic pulse light with peak wavelength of 590 nm should be higher than 14.4 mW cm^2, with the assumption of 50% external quantum efficiency [45]. The calculated value of critical light intensity (14.4 mW cm^2) is in agreement with the experimental value of 17.6 mW cm^2 required as a minimal intensity to generate charge accumulation.

We further discuss the effects of interfacial dipoles on bulk charge accumulation. As shown in Fig. 2d, the $\tau_{1/e}$ for Al device is larger than that of Ca device at constant pulse intensity, implying that interface can influence charge accumulation within the BHJ layer. This can be further proved by comparing the absolute amount of the extracted charges. By integrating the decay curves of transient photocurrent after the turn-off of pulse light, the absolute amount of the extracted charges is quantified and shown in Fig. 2c at different pulse intensities. In general, the extracted charges can be divided into two parts: photogenerated free carriers, responsible for external photocurrent, and the accumulated carriers, accountable for the space charges. In the case of weak pulse (shown in Fig. 1c), very similar quantities of accumulated charges are obtained for both Al and Ca devices at constant pulse intensity, suggesting that the extracted charges are mainly free photogenerated carriers and charge accumulation is negligible. However, in the case of strong pulse, as shown in Fig. 2c, more charges are extracted from Al device as compared to Ca device, indicating that a more serious accumulation of charges occurs in Al device. This experimental observation directly confirms that the improved interface can decrease the bulk charge accumulation inside the devices.

Here, we further discuss the influence of charge accumulation on charge extraction. As shown in insets of Fig. 2a and b, the decay of the photocurrent becomes slower with increasing pulse intensity for both Al and Ca devices. This experimental observation is completely different from the previous reports that a higher intensity corresponds to a faster decay owning to dominant trapping/detrapping effects in a polymer/polymer system [32,36]. In our devices, the photocurrent decay dynamics are controlled by the space charges generated by charge accumulation. Increasing the pulse intensity results in higher space charge density and thus retards the

photocurrent decay as shown in the insets of Fig. 2a and b. We also can see from insets of Fig. 2a and b that the Al and Ca devices share similar rise dynamics that is nearly independent on the pulse intensity. However, the rise time, defined as the time taken to the 90% of the saturation current, is slightly different, which are 6 μs for Al device and 4 μs for Ca device, respectively. This is because that Al cathode leads to a more serious charge accumulation and thus corresponds to a screened driving force for carriers transporting. As a result, the Ca device exhibits a higher carrier drift velocity and thus a faster rise response than that with Al electrode. These experimental observations provide direct evidence that a serious charge accumulation can slow down charge extraction.

The published results have shown that charge trapping in a polymer/polymer system also plays an important role in determining the photocurrent kinetics [29,34]. However, our results indicate that trapping effects can be ignored. To confirm this argument, we further verify the influence of background continuous light on the photocurrent dynamics. Fig. 3 shows the transient photocurrent for a constant pulse intensity of 24.5 mW cm^{-2} with different background light intensities. If charge extraction is limited by trapping, altering the background light intensity should significantly influence the rise/decay kinetics through changing the occupation density of trapped charge [29]. However, we can see from the insets in Fig. 3a and b that both Al and Ca devices exhibit similar characteristics in transient photocurrent. The rise/decay kinetics are nearly independent on the pulse intensity, indicating that trapping effects are negligible for P3HT:PCBM film. Therefore, we can attribute the space charges distributed inside the P3HT:PCBM film mainly to the accumulation of photogenerated carriers in the bulk film.

Finally, the interfacial dipole effects on charge recombination are explored by examining the photoconductivity response approaching open-circuit (V_{oc}) condition. At V_{oc} condition no photogenerated carriers are extracted and consequently the charge recombination becomes dominant. Thus, measuring the transient photocurrent near the V_{oc} condition can provide the information on interfacial effects of charge recombination [46]. In OSCs, the recombination of two mobile carriers is a bimolecular process, which results in a power law dependence of photoconductivity on time [47]. While the recombination of a mobile carrier with trapped charge exhibit monomolecular property, which leads to an exponential decay [48]. Fig. 4a presents the transient photoconductivity data with an applied bias of 0.6 V. The linear decay of the photoconductivity in semi-logarithm scale suggests that the charge recombination undergoes a monomolecular process. The recombination time constants, defined as the time for the photoconductivity to decay to 1/e of its peak value, are obtained from linear least-squares fit of the photoconductivity data, which are 8.0 μs and 7.3 μs for Ca and Al devices, respectively (More details can be seen in Supporting Information). This is because in the presence of charge accumulation, the local accumulated charges act as a recombination center. The local accumulated charges can essentially recombine with the mobile charges, leading to a monomolecular recombination. As a result, the density of accumulated charges is the key factor determining the carrier loss within the active layer in the generation of photocurrent. This is further supported by the dependence of peak/steady short-circuit photocurrent on pulse intensity. As shown in Fig. 4b, a linear dependence is observed when charge accumulation is avoided by utilizing weak pulse intensity. While the dependence becomes nonlinear when charge accumulation take places by using strong pulse intensity (Fig. 4c), because the stronger charge accumulation causes a more serious loss in short-circuit photocurrent. All these results clearly indicate that the Al device exhibits a more serious accumulation of bulk charge carriers than the Ca device. Therefore, our results demonstrate that improved interface could decrease the charge recombination by reducing the charge accumulation within the active layer.

To confirm our above discussions that low work-function Ca can simultaneously improve both the interfacial and bulk properties, devices with model structure of ITO/PEDOT:PSS/P3HT:PCBM/cathode is fabricated with Al or Ca cathode. Fig. 5 shows the current–voltage (J–V) characteristics of P3HT/PCBM devices under AM 1.5G simulated solar illumination of 100 mW cm^{-2}. As expected, the device with Ca cathode exhibit a higher J_{sc} of 9.63 mW cm and a larger FF of 67.51%, which eventually lead to

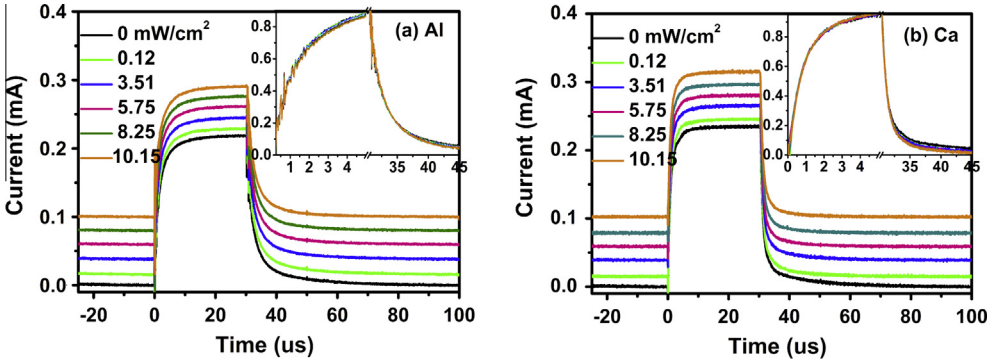

Fig. 3. Influence of background light intensity on photocurrent dynamics for a constant pulse intensity of 24.5 mW cm^{-2} for (a) Al and (b) Ca devices. The insets in part 3a and 3b exhibit the rise/decay dynamics by subtracting the background contribution.

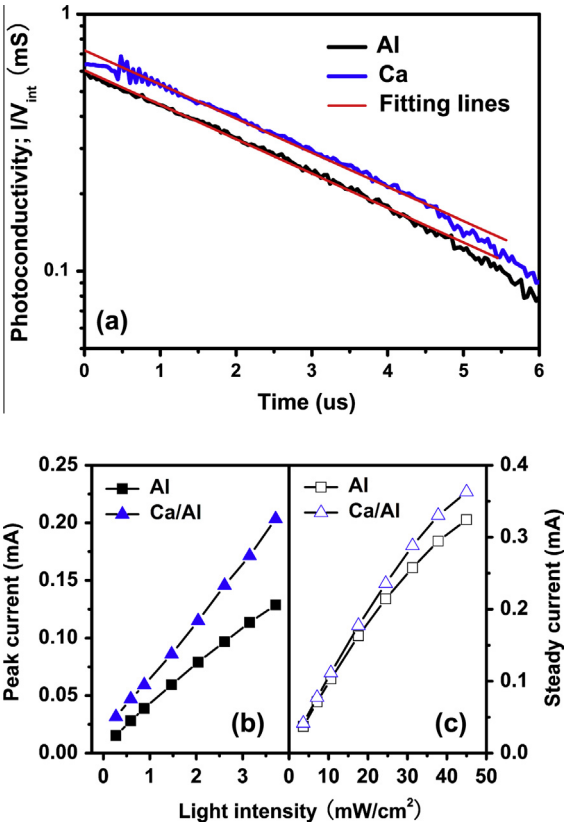

Fig. 4. (a) Transient photoconductance of Al (black line) and Ca (blue line) devices at small internal effective voltage of 0.067 V (V = 0.6 V) in a log-linear scale. The exciting pulse intensity is set at 45 mW cm^{-2} The red lines represent the fitted curves by using the equation $n(t) = n_0 * e^{t/\tau}$. (b) Peak short-circuit photocurrent deduced from Fig. 1a is shown as a function of pulse intensity. (c) Steady short-circuit photocurrent deduced from Fig. 2a is plotted as a function of pulse intensity. (For interpretation of the references to color in this figure legend, the reader is referred to the web version of this article.)

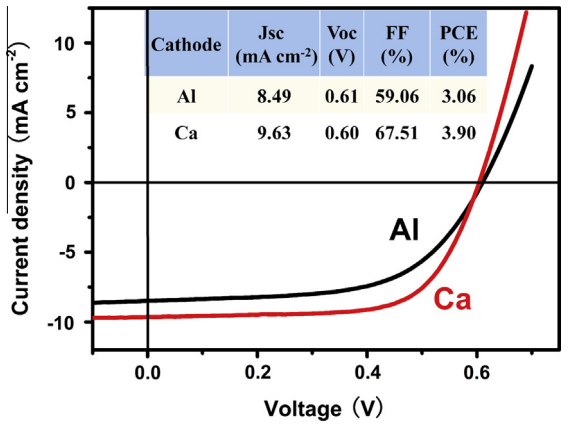

Fig. 5. Steady-state current–voltage characteristics of P3HT:PCBM devices with Al (black line) or Ca (red line) as cathode under AM 1.5G 100 mW cm^2 illumination. The inset presents the summary of device performance. (For interpretation of the references to color in this figure legend, the reader is referred to the web version of this article.)

the dramatic improvement in PEC by 27.5%. [42] On contrast, the J_{sc}. and *FF* for Al devices have lower values (J_{sc} = 8.49 mA cm^{-2}, *FF* = 59.06). These results demonstrate that the Ca electrode not only increases interfacial charge collection efficiency, but also decreases the charge recombination in the bulk layer, leading to improved J_{sc} and *FF*.

4. Conclusions

In summary, by using in situ transient photocurrent measurements, we studied the effects of interfacial dipoles on charge extraction, accumulation, and recombination based on bulk-heterojunction P3HT:PCBM system by comparing Ca and Al devices. The transient photocurrent measurements reveal that stronger interfacial dipoles can largely increase the charge extraction efficiency by reducing the charge extraction time. More importantly, we found that stronger interfacial dipoles can also decrease the charge accumulation within the bulk layer. Because the bulk-accumulated charges can act as recombination centers, decreasing the bulk accumulation can reduce the recombination loss in photogenerated carriers. Our results provide direct experimental evidence for the physical picture how the interfacial dipole affect the interfacial and bulk photovoltaic processes. Clearly, our studies of transient photocurrents elucidated the charge extraction, accumulation, and recombination in OSCs.

Acknowledgements

This research was supported by National Significant Program (Quantum Control: 2014CB643506, 2013CB922104) and International Cooperation and Exchange Program (Gant No. 21161160445). The author (X. Qiao) also acknowledge the supports from National Natural Science Foundation of China (No. 61205034) and China Postdoctoral Science Foundation (Grant No. 20110491143).

Appendix A. Supplementary material

Supplementary data associated with this article can be found, in the online version, at http://dx.doi.org/10.1016/j.orgel.2014.04.019.

References

[1] G. Yu, J. Gao, J.C. Hummelen, F. Wudl, A.J. Heeger, Science 270 (1995) 1789–1791.
[2] J.J.M. Halls, C.A. Walsh, N.C. Greenham, E.A. Marseglia, R.H. Friend, S.C. Moratti, A.B. Holmes, Nature 376 (1995) 498–500.
[3] T. Ameri, P. Khoram, J. Min, C.J. Brabec, Adv. Mater. 25 (2013) 4245–4266.
[4] J.B. You, L.T. Dou, K. Yoshimura, T. Kato, K. Ohya, T. Moriarty, K. Emery, C.C. Chen, J. Gao, G. Li, Y. Yang, Nat. Commun. 4 (2013) 1446.
[5] P.D. Homyak, J. Tinkham, P.M. Lahti, E.B. Coughlin, Macromolecules 46 (2013) 8873–8881.
[6] C.M. Amb, S. Chen, K.R. Graham, J. Subbiah, C.E. Small, F. So, J.R. Reynolds, J. Am. Chem. Soc. 133 (2011) 10062–10065.
[7] J.M. Jiang, M.C. Yuan, K. Dinakaran, A. Hariharan, K.H. Wei, J Mater. Chem. A 14 (2013) 4415–4422.
[8] Y.J. He, H.-Y. Chen, J.H. Houand, Y.F. Li, J. Am. Chem. Soc. 132 (2010) 1377.

[9] H.Y. Lv, X.L. Zhao, W.T. Xu, H. Li, J. Chen, X.N. Yang, Org. Electron. 14 (2013) 1874–1881.
[10] C.M. Liu, M.S. Su, J.M. Jiang, Y.W. Su, C.J. Su, C.Y. Chen, C.S. Tsao, K.H. Wei, ACS Appl. Mater. Int. 5 (2013) 5413–5422.
[11] Y.-C. Huang, H.-C. Chia, C.-M. Chuang, C.-S. Tsao, C.-Y. Chen, W.-F. Su, Sol. Energy Mater. Sol. Cells 114 (2013) 24–30.
[12] C.M. Liu, C.Y. Chen, Y.W. Su, S.M. Wang, K.H. Wei, Org. Electron. 14 (2013) 2476–2483.
[13] F.-X. Xie, W.C.H. Choy, W.E.I. Sha, D. Zhang, S. Zhang, X. Li, C.-W. Leungand, J.-H. Hou, Energy Environ. Sci. 6 (2013) 3372–3379.
[14] Z.C. He, C.M. Zhong, X. Huang, W.Y. Wong, H.B. Wu, L.W. Chen, S.J. Su, Y. Cao, Adv. Mater. 23 (2011) 4636–4643.
[15] Y.H. Zhou, C. Fuentes-Hernandez, J. Shim, J. Meyer, A.J. Giordano, H. Li, P. Winget, T. Papadopoulos, H. Cheun, J. Kim, M. Fenoll, A. Dindar, W. Haske, E. Najafabadi, T.M. Khan, H. Sojoudi, S. Barlow, S. Graham, J.-L. Brédas, S.R. Marder, A. Kahn, B. Kippelen, Science 336 (2012) 327–332.
[16] Y. Jouane, S. Colis, G. Schmerber, A. Dinia, P. Lévêque, T. Heiser, Y.-A. Chapuis, Org. Electron. 14 (2013) 1861–1868.
[17] S. Höfle, H. Do, E. Mankel, M. Pfaff, Z. Zhang, D. Bahro, T. Mayer, W. Jaegermann, Org. Electron. 14 (2013) 1820–1824.
[18] T.B. Yang, M. Wang, C.H. Duan, X.W. Hu, L. Huang, J.B. Peng, F. Huang, X. Gong, Energy Environ. Sci. 5 (2012) 8208–8214.
[19] B.B. Chen, X.F. Qiao, C.-M. Liu, C. Zhao, H.-C. Chen, K.-H. Wei, B. Hu, Appl. Phys. Lett. 102 (2013) 193302.
[20] T.M. Clarke, J.R. Durrant, Chem. Rev. 110 (2010) 6736–6767.
[21] Y.J. Cheng, S.H. Yang, C.S. Hsu, Chem. Rev. 109 (2009) 5868.
[22] A.-L. Shi, Y.-Q. Li, Z.-Q. Xu, F.-Z. Sun, J. Li, X.-B. Shi, H.-X. Wei, S.-T. Lee, S. Kera, Org. Electron. 14 (2013) 1844–1851.
[23] A.J. Mozer, G. Dennler, N.S. Sariciftci, M. Westerling, A. Pivrikas, R. Österbacka, G. Juška, Phys. Rev. B 72 (2005) 035217.
[24] G. Dennler, A.J. Mozer, G. Juška, A. Pivrikas, R. Österbacka, A. Fuchsbauer, N.S. Sariciftci, Org. Electron. 7 (2006) 229–234.
[25] R. Hanfland, M.A. Fischer, W. Brütting, U. Würfel, R.C.I. Mackenzie, Appl. Phys. Lett. 103 (2013) 063904.
[26] A. Baumann, T.J. Savenije, D.H.K. Murthy, M. Heeney, V. Dyakonov, C. Deibel, Adv. Funct. Mater. 21 (2011) 1687–1692.
[27] C.G. Shuttle, B. O'Regan, A.M. Ballantyne, J. Nelson, D.D.C. Bradley, J. de Mello, J.R. Durrant, Appl. Phys. Lett. 92 (2008) 093311.
[28] A. Maurano, C.G. Shuttle, R. Hamilton, A.M. Ballantyne, J. Nelson, W.M. Zhang, M. Heeney, J.R. Durrant, J. Phys. Chem. C 115 (2011) 5947–5957.
[29] Z. Li, F. Cao, N.C. Creenham, C.R. McNeill, Adv. Funct. Mater. 21 (2011) 1419–1431.
[30] A. Armin, G. Juska, B.W. Philippa, P.L. Burn, P. Meredith, R.D. White, A. Pivrikas, Adv. Energy Mater. 3 (2013) 321–325.
[31] P. Chen, J.H. Huang, Z.H. Xiong, F. Li, Org. Electron. 14 (2013) 621–627.
[32] Y.-S. Kim, T. Kim, B. Kim, D.-K. Lee, H. Kim, B.-K. Ju, K. Kim, Org. Electron. 14 (2013) 1749–1754.
[33] A. Foertig, A. Baumann, D. Rauh, V. Dyakonov, C. Deibel, Appl. Phys. Lett. 95 (2009) 052104.
[34] T. Leijtens, J. Lim, J. Teuscher, T. Park, H.J. Snaith, Adv. Mater. 25 (2013) 3227–3232.
[35] I. Hwang, C.R. McNeill, N.C. Greenham, J. Appl. Phys. 106 (2009) 094506.
[36] W. Tress, S. Corvers, K. Leo, M. Riede, Adv. Energy Mater. 3 (2013) 873–880.
[37] Z. Li, C.R. McNeill, J. Appl. Phys. 109 (2011) 074513.
[38] A. Baumann, J. Lorrmann, D. Rauh, C. Deibel, V. Dyakonov, Adv. Mater. 24 (2012) 4381–4386.
[39] R.C.I. MacKenzie, C.G. Shuttle, M.L. Chabinyc, J. Nelson, Adv. Energy, Mater. 2 (2012) 662–669.
[40] L.M. Chen, Z. Xu, Z.R. Hong, Y. Yang, J. Mater. Chem. 20 (2010) 2575–2598.
[41] W.-H. Tseng, M.-H. Chen, J.-Y. Wang, C.-T. Tseng, H. Lo, P.-S. Wang, C.-I Wu, Sol. Energy Mater. Sol. Cells 95 (2011) 3424.
[42] Y. Yi, S.J. Kang, Thin Solid Film 519 (2006) 3119–3122.
[43] H. Ishii, K. Sugiyama, E. Ito, K. Seki, Adv. Mater. 11 (1999) 605–625.
[44] G. Li, V. Shrotriya, J.S. Huang, Y. Yao, T. Moriarty, K. Emery, Y. Yang, Nat. Mater. 4 (2005) 864–868.
[45] Y.J. Cho, J.Y. Lee, B.D. Chin, S.R. Forrest, Org. Electron. 14 (2013) 1081–1085.
[46] R.A. Street, S.R. Cowan, A.J. Heeger, Phys. Rev. B 82 (2010) 121301.
[47] A. Foertig, A. Wagenpfahl, T. Gerbich, D. Cheyns, V. Dyakonov, C. Deibel, Adv. Energy Mater. 2 (2012) 1483–1489.
[48] S.R. Cowan, R.A. Street, S. Cho, A.J. Heeger, Phys. Rev. B 83 (2011) 035205.